The object of this study is the control of quadrotor. Unmanned aerial vehicles currently in use often encounter various challenges and limitations. When operating in environments affected by external disturbances-particularly, when carrying suspended loads via cables, the control problem becomes significantly more complex. As a result, the quadrotor is unable to accurately follow the predefined flight trajectory.

Problem that was solved is the synthesis of a new controller for the quadrotor with a cable-suspended load, ensuring that the quadrotor accurately follows the predefined flight trajectory. The proposed algorithm demonstrates a significant improvement over existing methods by effectively suppressing the oscillation angle of the suspended payload, treating the payload's influence as an external disturbance. Furthermore, it constrains the swing angle within an acceptable range, thereby ensuring the stability and robustness of the overall system during operation.

This study presents a novel control algorithm capable of guiding the quadrotor precisely to the desired position, even under the condition of carrying a cable-suspended load in a varying environment. The algorithm demonstrates a significant advantage, enabling the quadrotor to reach the desired trajectory within 2.6 seconds. The suspended load exhibits only small oscillations, which gradually diminish as the quadrotor transitions to a stable state. With its simple structure, high stability, and fast convergence, this robust solution is essential for unmanned aerial vehicles, significantly enhancing their operational effectiveness under complex conditions.

A key strength of the proposed algorithm lies in its simple structure. Furthermore, it demonstrates high convergence rates and exceptional stability, crucial attributes for real-time applications. Its design also ensures ease of practical implementation, making it a viable solution for unmanned aerial vehicles.

The algorithm is developed based on modern control techniques, combining a sliding mode controller with an extended state observer. The SMC maintains system stability in the presence of disturbances and uncertainties, while the ESO estimates unmeasured states and aggregated disturbances affecting the system. This design ensures accurate positioning of the quadrotor with a suspended load at the desired location

Keywords: sliding mode control, extended state observer, unmanned aerial vehicle, trajectory

UDC 629.735:681.5

DOI: 10.15587/1729-4061.2025.342109

SYNTHESIS OF A CONTROLLER FOR QUADROTORS WITH SUSPENDED PAYLOADS

Nguyen Thi Dieu Linh
Corresponding author
PhD
Department of Science and Technology
Hanoi University of Industry
Cau Dien str., 298, Hanoi,
Vietnam, 100000
E-mail: nguyen.linh@haui.edu.vn

Nguyen Van Bang
PhD
Department of Missile
Air Defence – Air Force Academy
Kim Son str., 29, Hanoi,
Vietnam, 100000

Received 04.08.2025
Received in revised form 06.10.2025
Accepted 16.10.2025
Published 31.10.2025

How to Cite: *Linh, N. T. D., Bang, N. V. (2025). Synthesis of a controller for quadrotors with suspended payloads. Eastern-European Journal of Enterprise Technologies, 5 (7 (137)), 65–71. https://doi.org/10.15587/1729-4061.2025.342109*

1. Introduction

Unmanned aerial vehicles (UAVs) are being increasingly utilized in various sectors, including military operations, transportation, agriculture, and search and rescue [1]. Among the different configurations, the quadrotor is particularly popular due to its simple design, high maneuverability, and ability to operate effectively in confined spaces [2]. When equipped with a suspended payload, these systems can perform tasks in hard-to-reach areas that are inaccessible to conventional transport vehicles [3]. However, controlling such a system presents significant technical challenges.

Quadrotor systems with suspended payloads often face complex problems such as payload oscillations [4], external disturbances from factors like wind or environmental changes, model uncertainties, and sensor errors [5]. The additional degrees of freedom introduced by the suspended cable further complicates the control problem [6]. Moreover, in tropical monsoon environments, the electronic components of the control system are prone to degradation, which can compromise reliability and operational efficiency [7]. To ensure stable quadrotor operation under these diverse and challenging conditions, there is a critical need for advanced control systems that exhibit high reliability, strong adaptability, and sufficient robustness. Therefore, research on the development of unmanned aerial vehicles for quadrotors with suspended payloads is highly relevant.

2. Literature review and problem statement

One of the most significant capabilities of quadrotors is their potential for transportation in various fields. To carry loads, quadrotors can employ two primary methods [8]. Directly attaching the payload to the frame, or suspending it via a cable.

Direct attachment method usually employs mechanical fixtures or electromagnets. These attachment mechanisms increase the total system mass, rotational inertia, and energy consumption [9]. Moreover, this method is limited in handling large payloads since it must preserve the center-of-mass balance [10].

Cable suspension method offers a simpler design, reduces system weight, avoids adding extra rotational inertia, and is generally more cost-efficient than direct attachment [11]. However, its limitation lies in payload oscillations, which may compromise quadrotor safety [12].

A quadrotor-payload system with cable suspension separates the payload from the frame, allowing transport of larger objects compared to direct attachment. This mechanism is

advantageous in construction, where it facilitates the delivery of materials and tools to elevated or hard-to-reach areas [13]. In rescue operations, the system can precisely drop supplies to victims without landing, which is suitable for rugged terrain or water surfaces. Additionally, in surveying and measurement tasks, maintaining a fixed suspension length ensures that sensors and measuring devices are unaffected by rotor airflow or electromagnetic interference, thereby improving measurement accuracy [14].

Nonetheless, payload oscillations are unavoidable in cable-suspended systems and negatively impact stability. Determining the swing angle of the payload is thus essential for providing feedback to the controller to suppress oscillations and stabilize the quadrotor during operation. Methods for determining payload swing angles can be classified into two main groups [15]:

1. Estimation methods. These do not require direct measurement. Instead, they employ dynamic models or fuse available sensor data to compute the swing angle.

2. Direct measurement methods are divided into contact-based and non-contact-based approaches:

– contact-based: sensors are mounted on the suspension cable or directly on the payload. Cable-mounted sensors may include potentiometers (simple but environmentally sensitive) or rotary encoders (offering higher resolution and accuracy). Payload-mounted sensors include inclinometers, inertial sensors, or attitude and heading reference sensors;

– non-contact-based: these mainly involve two techniques. The first uses laser displacement sensors and reflective targets mounted on the cable to measure relative distance and calculate swing angle. The second employs monocular or multi-camera systems to determine payload position and swing angle. The major advantage of non-contact methods is that they require no modification of the mechanical suspension structure; however, they are generally more complex and costly.

Typically, quadrotor controllers require multiple sensors to compare reference and actual signals in order to generate appropriate control actions, which increases system complexity and cost.

The paper [15] It is shown that controllers designed using Lyapunov functions ensure the stability of desired trajectories along the (X, Z) axes and tilt angles. PID and LQR controllers are applied to stabilize altitude [16]. While DC actuators combined with adaptive controllers are employed to stabilize motion [17]. But there are still unresolved questions related to disturbances. The reasons of it can be the state of the controller has changed, and it is no longer linear, which makes the corresponding researches inexpedient. Under strong disturbances, these controllers lose linearity, and closed-loop stability can only be maintained in a small region around equilibrium.

The paper [18] It is shown that other methods include fuzzy logic control and neural networks, which aim to drive Euler angles toward zero during motion. Sliding mode control (SMC) and higher-order SMC [19, 20] have also been used to estimate unmeasured state variables and reject external disturbances such as wind or noise. But there are still unresolved questions related to estimate unmeasured state variables. Nonetheless, these controllers often require extensive and complex computations.

From these considerations, this paper proposes a method to design and simulate a quadrotor control system with a suspended payload attached by a cable of fixed length. The approach is based on combining SMC with an extended state observer (ESO). The SMC maintains system stability in the presence of disturbances and uncertainties, while the ESO estimates unmeasured states and aggregated disturbances affecting the system, thereby enhancing control performance. This control structure is well-suited for quadrotor-payload systems operating under real-world conditions.

All this allows to assert that it is expedient to conduct a study on the synthesis of a new controller for a quadrotor with a suspended load.

3. The aim and objectives of the study

The aim of this study is to develop a highly efficient, robust, and adaptive control solution for UAVs carrying cable-suspended loads, thereby significantly enhancing their performance, stability, and reliability to support critical applications such as cargo transportation, surveillance, rescue operations, and missions in complex environments.

To achieve this aim, the following three specific objectives were accomplished:

– to design and develop a novel control algorithm by integrating a SMC and an ESO capable of accurately controlling a quadrotor with a suspended load to follow a predefined flight trajectory;

– to implement and validate the model's robustness, demonstrating the algorithm's capability to successfully control the quadrotor and suspended load along complex trajectories while maintaining stable operation under varying environmental conditions;

– to quantify the performance of the developed algorithm, specifically achieving near-zero steady-state error and high convergence and to attribute this performance to the algorithm's simple structure and exceptional stability.

4. Materials and methods

4. 1. The object and hypothesis of the study

The object of this study is the control of quadrotor.

The hypothesis suggests the possibility of finding a solution for effective control of quadrotor equipped with a suspended load using a fixed, inextensible cable.

Mathematical modeling was carried out using the MATLAB software environment.

The cable-suspension method with fixed length is simple in terms of mechanical design but poses significant challenges in flight control. This is because quadrotors are affected by payload oscillations during flight and by dynamic changes when the cable transitions between taut and slack states. These factors influence quadrotor stability and its ability to track predefined flight trajectories. Therefore, developing effective control methods to mitigate payload-induced oscillations is an important issue in cable-suspended quadrotor applications.

In [21], a quadrotor-payload model was constructed using the Lagrangian method, with eight degrees of freedom: six corresponding to the basic quadrotor motion and two representing payload swing angles. A backstepping controller was then proposed.

In this paper, the payload is modeled as a spherical pendulum, with particular attention given to the forces exerted on the quadrotor's position due to payload motion. The controller is designed to regulate quadrotor position under the influence of payload swing, enabling it to follow predefined trajectories.

To analyze the dynamics of the cable-suspended quadrotor system, the following assumptions are adopted [22]:

Assumption 1: The suspension point is located at the center of mass of the quadcopter.

Assumption 2: The suspension system is frictionless, and air resistance is neglected.

Assumption 3: The cable is massless and inextensible.

To determine the payload position, a new coordinate system {H} is introduced, with its origin at the suspension point, as shown in Fig. 1.

Angles α and β denote the swing angles between the cable and the *Hy-Hz* plane, and the *Hx-Hz* plane, respectively. In the ground-fixed reference frame, the payload position is expressed as

$$P_l = \begin{bmatrix} x_l \\ y_l \\ z_l \end{bmatrix} = \begin{bmatrix} x + LS_\beta \\ y + LS_\alpha C_\beta \\ z - LC_\alpha C_\beta \end{bmatrix}, \quad (1)$$

where $S_\beta = \sin\beta$, $C_\alpha = \cos\alpha$.

The first- and second-order derivatives of equation (1) yield:

$$\dot{P}_l = \begin{bmatrix} \dot{x}_l \\ \dot{y}_l \\ \dot{z}_l \end{bmatrix} = \begin{bmatrix} \dot{x} + LC_\beta\dot{\beta} \\ \dot{y} - L\left(S_\beta S_\alpha\dot{\beta} - C_\beta C_\alpha\dot{\alpha}\right) \\ \dot{z} + L\left(S_\beta C_\alpha\dot{\beta} + C_\beta S_\alpha\dot{\alpha}\right) \end{bmatrix}, \quad (2)$$

$$\ddot{P}_l = \begin{bmatrix} \ddot{x}_l \\ \ddot{y}_l \\ \ddot{z}_l \end{bmatrix} = \begin{bmatrix} \ddot{x} + L\left(\ddot{\beta}C_\beta - \dot{\beta}^2 S_\beta\right) \\ \ddot{y} + L\begin{pmatrix} -\ddot{\beta}S_\beta S_\alpha + \ddot{\alpha}C_\beta C_\alpha - \\ -\dot{\beta}^2 C_\beta S_\alpha - \dot{\alpha}^2 C_\beta S_\alpha - 2\dot{\beta}\dot{\alpha}S_\beta C_\alpha \end{pmatrix} \\ \ddot{z} + L\begin{pmatrix} \ddot{\beta}S_\beta C_\alpha + \ddot{\alpha}C_\beta S_\alpha + \\ +\dot{\beta}^2 C_\beta C_\alpha + \dot{\alpha}^2 C_\beta C_\alpha - 2\dot{\beta}\dot{\alpha}S_\beta S_\alpha \end{pmatrix} \end{bmatrix}. \quad (3)$$

Considering gravitational force acting on the suspended payload

$$F_g = \begin{bmatrix} 0 & 0 & -\left(m_q + m_l\right) \end{bmatrix}^T.$$

The forces acting on the quadrotor, together with disturbances, can be written using the Newton-Euler formulation

$$F - F_G - F_D + D_1 = m_q \cdot \ddot{P} + m_l \cdot \ddot{P}_l, \quad (4)$$

where P and P_l are the positions of the quadrotor and the payload, m_q is the quadrotor mass, m_l is the payload mass.

From (3), (4), the kinematic model of the quadrotor with suspended payload is derived as

$$\begin{cases} \ddot{x} = \dfrac{F_x - m_l L\left(\ddot{\beta}C_\beta - \dot{\beta}^2 S_\beta\right) - k_{cx}\dot{x} + D_x}{m}; \\ \ddot{y} = \dfrac{F_y - m_l L\left(-\ddot{\beta}S_\beta S_\alpha + \ddot{\alpha}C_\beta C_\alpha - \dot{\beta}^2 C_\beta S_\alpha - \dot{\alpha}^2 C_\beta S_\alpha - 2\dot{\beta}\dot{\alpha}S_\beta C_\alpha\right) - k_{cy}\dot{y} + D_y}{m}; \\ \ddot{z} = \dfrac{F_z - m_l L\left(\ddot{\beta}S_\beta C_\alpha + \ddot{\alpha}C_\beta S_\alpha + \dot{\beta}^2 C_\beta C_\alpha + \dot{\alpha}^2 C_\beta C_\alpha - 2\dot{\beta}\dot{\alpha}S_\beta S_\alpha\right) - k_{cz}\dot{z} + D_z}{m} - g; \\ \ddot{\phi} = \dfrac{M_\phi}{I_{xx}} + \dfrac{\left(I_{yy} - I_{zz}\right)}{I_{xx}}\dot{\theta}\dot{\psi} - \dfrac{k_{d\phi}}{I_{xx}}\dot{\phi}^2 + \dfrac{D_\phi}{I_{xx}}; \\ \ddot{\theta} = \dfrac{M_\theta}{I_{yy}} + \dfrac{\left(I_{xx} - I_{zz}\right)}{I_{yy}}\dot{\psi}\dot{\phi} - \dfrac{k_{d\theta}}{I_{yy}}\dot{\theta}^2 + \dfrac{D_\theta}{I_{yy}}; \\ \ddot{\psi} = \dfrac{M_\psi}{I_{zz}} + \dfrac{\left(I_{xx} - I_{yy}\right)}{I_{zz}}\dot{\phi}\dot{\theta} - \dfrac{k_{d\phi}}{I_{zz}}\dot{\psi}^2 + \dfrac{D_\psi}{I_{zz}}, \end{cases} \quad (5)$$

where $m = m_l + m_q$ is the total mass of the quadrotor and payload;

k_{ci} and k_{di} are drag coefficients.

According to model (5), the translational acceleration of the quadrotor is directly coupled with the payload swing angles. Large oscillations of the payload significantly affect quadrotor position. Therefore, separate control of quadrotor position and payload swing angles is required, such that the system not only tracks the desired trajectory but also minimizes payload oscillations during flight.

The total energy of the system is derived from Hamilton's principle and the Lagrangian equations [23]

$$\frac{d}{d\tau}\left(\frac{\partial\left(T-P\right)}{\partial\dot{q}_k}\right) - \left(\frac{\partial\left(T-P\right)}{\partial q_k}\right) = 0, \quad (6)$$

where T is the total kinetic energy, P is the potential energy, and q_k denotes generalized coordinates (here, α and β).

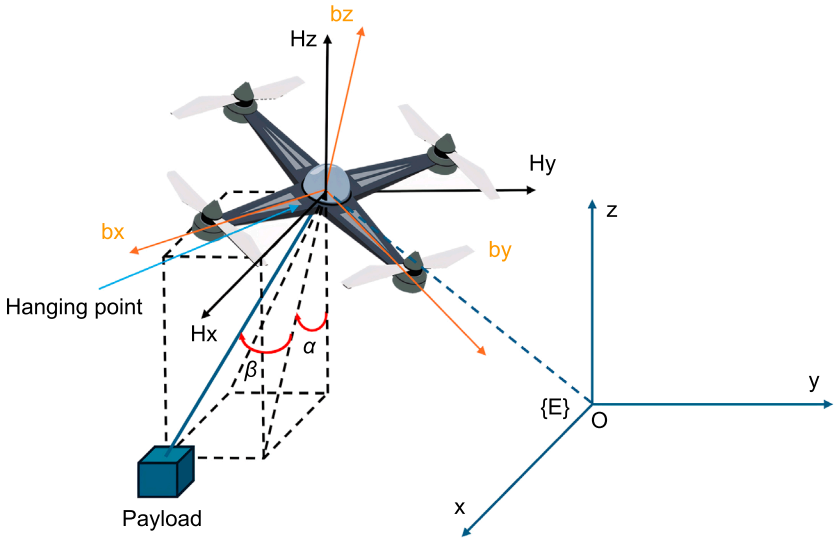

Fig. 1. Dynamic model of a quadrotor with suspended payload

From (1) and (2), the kinetic and potential energies are obtained as:

$$\begin{aligned}T=&\frac{1}{2}m_q\left(\dot{x}^2+\dot{y}^2+\dot{z}^2\right)+\\&+\frac{1}{2}m_l\left(\dot{x}_l^{\,2}+\dot{y}_l^{\,2}+\dot{z}_l^{\,2}\right)=\\&=\frac{1}{2}m_q\left(\dot{x}^2+\dot{y}^2+\dot{z}^2\right)+\\&+\frac{1}{2}m_l\begin{bmatrix}\left(\dot{x}+LC_\beta\dot{\beta}\right)^2+\\+\left(\dot{y}-L\left(S_\beta S_\alpha\dot{\beta}-C_\beta C_\alpha\dot{\alpha}\right)\right)^2+\\+\left(\dot{z}+L\left(S_\beta C_\alpha\dot{\beta}+C_\beta S_\alpha\dot{\alpha}\right)\right)^2\end{bmatrix};\end{aligned}\tag{7}$$

$$P=\left(m_l+m_q\right)gz-m_lgLC_\alpha C_\beta.\tag{8}$$

Substituting (7) and (8) into (6), and considering $q_k=\alpha,\beta$. The relationship between payload swing accelerations and quadrotor translational accelerations can be derived as

$$\begin{cases}L\ddot{\beta}+C_\beta\ddot{x}-S_\beta S_\alpha\ddot{y}+\\+S_\beta C_\alpha\ddot{z}+LS_\beta C_\beta\dot{\alpha}^2+gS_\beta C_\alpha=0;\\C_\beta\ddot{\alpha}+C_\alpha\ddot{y}+S_\alpha\ddot{z}-\\-2LS_\beta\dot{\beta}\dot{\alpha}+gS_\alpha=0.\end{cases}\tag{9}$$

Thus, from and , the dynamics of payload swing angles are obtained as

$$\begin{cases}\ddot{\alpha}=\dfrac{2\left(m_q+m_l\right)LS_\beta\dot{\beta}\dot{\alpha}-C_\alpha F_y-S_\alpha F_z}{(m_q+m_l)Lc_\beta};\\\ddot{\beta}=\\=\dfrac{-\left(m_q+m_l\right)LS_\beta C_\beta\dot{\alpha}^2-C_\beta F_x-S_\beta S_\alpha F_y-S_\beta C_\alpha F_z}{\left(m_q+m_l\right)L}.\end{cases}\tag{10}$$

Thus, in this section, it is developed the kinematic model of the quadrotor with a suspended load under the condition of a fixed cable length.

5. Results of development of the method of quadrotor with fixed-length cable suspension

5. 1. A new controller for quadrotor with fixed-length cable suspension

The dynamic model of a quadrotor, considering environmental disturbances, can be expressed as follows [15–20]

$$\begin{cases}\ddot{x}=b_xF_x+d_x;\\\ddot{y}=b_yF_y+d_y;\\\ddot{z}=b_zF_z+d_z;\\\ddot{\phi}=b_\phi M_\phi+d_\phi;\\\ddot{\theta}=b_\theta M_\theta+d_\theta;\\\ddot{\psi}=b_\psi U_\psi+d_\psi,\end{cases}\tag{11}$$

where U_x, U_y, U_z are translational control inputs, M_ϕ, M_θ, U_ψ are rotational inputs, b_i are system parameters, and d_i represent disturbances.

In the presence of payload oscillations, the effects of the suspended load are treated as external disturbances. Accordingly, the dynamic model in (5) can be rewritten in a similar form

$$\begin{cases}\ddot{x}=b'_xF_x+d'_x;\\\ddot{y}=b'_yF_y+d'_y;\\\ddot{z}=b'_zF_z+d'_z;\\\ddot{\phi}=b'_\phi M_\phi+d'_\phi;\\\ddot{\theta}=b'_\theta M_\theta+d'_\theta;\\\ddot{\psi}=b'_\psi M_\psi+d'_\psi.\end{cases}\tag{12}$$

Here, the parameters *b, d* are redefined:

$$\begin{bmatrix}b'_x & b'_y & b'_z & b'_\phi & b'_\theta & b'_\psi\end{bmatrix}^T=$$
$$=\begin{bmatrix}\frac{1}{m} & \frac{1}{m} & \frac{1}{m} & \frac{1}{I_{xx}} & \frac{1}{I_{yy}} & \frac{1}{I_{zz}}\end{bmatrix}^T;$$

$$\begin{bmatrix}d'_x\\d'_y\\d'_z\\d'_\phi\\d'_\theta\\d'_\psi\end{bmatrix}=$$

$$=\begin{bmatrix}\frac{D_x}{m}-\frac{k_{cx}\dot{x}}{m}-\frac{m_lL\left(\ddot{\beta}C_\beta-\dot{\beta}^2S_\beta\right)}{m}\\\frac{D_y}{m}-\frac{k_{cy}\dot{y}}{m}-\\-\frac{m_lL\left(-\ddot{\beta}S_\beta S_\alpha+\ddot{\alpha}C_\beta C_\alpha-\dot{\beta}^2C_\beta S_\alpha-\dot{\alpha}^2C_\beta S_\alpha-2\dot{\beta}\dot{\alpha}S_\beta C_\alpha\right)}{m}\\\frac{D_z}{m}-\frac{k_{cz}\dot{z}}{m}-\\-\frac{m_lL\left(\ddot{\beta}S_\beta C_\alpha+\ddot{\alpha}C_\beta S_\alpha+\dot{\beta}^2C_\beta C_\alpha+\dot{\alpha}^2C_\beta C_\alpha-2\dot{\beta}\dot{\alpha}S_\beta S_\alpha\right)}{m}-g\\\frac{\left(I_{yy}-I_{zz}\right)}{I_{xx}}\dot{\theta}\dot{\psi}-\frac{k_{d\phi}}{I_{xx}}\dot{\phi}^2+\frac{D_\phi}{I_{xx}}\\\frac{\left(I_{xx}-I_{zz}\right)}{I_{yy}}\dot{\psi}\dot{\phi}-\frac{k_{d\theta}}{I_{yy}}\dot{\theta}^2+\frac{D_\theta}{I_{yy}}\\\frac{\left(I_{xx}-I_{yy}\right)}{I_{zz}}\dot{\phi}\dot{\theta}-\frac{k_{d\psi}}{I_{zz}}\dot{\psi}^2+\frac{D_\psi}{I_{zz}}\end{bmatrix}.\tag{13}$$

Since the dynamic models (11), (12) share a similar structure, the trajectory-tracking controller for the quadrotor with suspended payload can be designed in the same way as for a system subjected to external disturbances. In other words, the payload oscillations are treated as external disturbances acting on the system.

Similarly, the ESO is designed as

$$\begin{cases} \dot{\hat{\chi}}_1 = \hat{\chi}_2 + \frac{\alpha_1}{\varepsilon}(\chi_1 - \hat{\chi}_1); \\ \dot{\hat{\chi}}_2 = bu + \hat{d}' + \frac{\alpha_2}{\varepsilon^2}(\chi_1 - \hat{\chi}_1); \\ \dot{\hat{d}}' = \frac{\alpha_3}{\varepsilon^3}(\chi_1 - \hat{\chi}_1), \end{cases} \quad (14)$$

where $\chi_1 = \{x, y, z, \Phi, \theta, \psi\}$, $a = \{a_x, a_y, a_z, a_\Phi, a_\theta, a_\psi\}$, $b = \{b_x, b_y, b_z, b_\Phi, b_\theta, b_\psi\}$, $u = \{U_x, U_y, U_z, U_\Phi, U_\theta, U_\psi\}$, $d = \{d'_x, d'_y, d'_z, d'_\phi, d'_\theta, d'_\psi\}$. The ESO aims to ensure that the estimated values converge to actual $\hat{\chi}_1 \to 1$, $\hat{\chi}_2 \to \hat{\chi}_2$, $\hat{d}' \to d'$ ones as $t \to \infty$.

To guarantee trajectory tracking $\{x_d, y_d, z_d, \psi_d\}$ even under payload-induced disturbances, a SMC is designed for position and attitude loops

$$\begin{cases} U_x = m\left(-\hat{d}'_x + \ddot{x}_d + c_x\dot{\hat{e}}_x + n_x sat(\hat{s}_x) + k_x\hat{s}_x\right); \\ U_y = m\left(-\hat{d}'_y + \ddot{y}_d + c_y\dot{\hat{e}}_y + n_y sat(\hat{s}_y) + k_y\hat{s}_y\right); \\ U_z = m\left(-\hat{d}'_z + \ddot{z}_d + c_z\dot{\hat{e}}_z + n_z sat(\hat{s}_z) + k_z\hat{s}_z\right); \\ U_\phi = I_{xx}\left(-\hat{d}'_\phi + \ddot{f}_d + c_\phi\dot{\hat{e}}_\phi + n_\phi sat(\hat{s}_\phi) + k_\phi\hat{s}_\phi\right); \\ U_\theta = I_{yy}\left(-\hat{d}'_\theta + \ddot{\theta}_d + c_\theta\dot{\hat{e}}_\theta + n_\theta sat(\hat{s}_\theta) + k_\theta\hat{s}_\theta\right); \\ U_\psi = I_{zz}\left(-\hat{d}'_\psi + \ddot{\psi}_d + c_\psi\dot{\hat{e}}_\psi + n_\psi sat(\hat{s}_\psi) + k_\psi\hat{s}_\psi\right), \end{cases} \quad (15)$$

where e_i are tracking errors; s_i are sliding surfaces; c_i, k_i, n_i are control gains, $\hat{d}_i$ are disturbance estimates provided by the ESO, I_{xx}, I_{yy}, I_{zz} are the inertia moments.

The total thrust and the desired attitude angles θ_d, ϕ_d are then determined by

$$\begin{cases} U_m = \sqrt{U_x^2 + U_y^2 + U_z^2}; \\ \theta_d = \\ = \arctan\left(\frac{U_x\cos\psi_d + U_y\sin\psi}{U_z}\right); \\ \phi_d = \\ = \arctan\left(\frac{U_x\sin\psi_d - U_y\cos\psi}{U_z}\cos\theta\right). \end{cases} \quad (16)$$

This control scheme ensures that the quadrotor follows the desired trajectory while actively compensating for payload oscillations considered as external disturbances.

5. 2. Simulation parameters

In this section, simulations are conducted for a quadrotor carrying a suspended payload with a fixed cable length of 0.25 (m) and a payload mass of 0.5 (kg). Since the rotational dynamics remain unchanged, the focus here is on position tracking and payload swing angles.

The reference trajectory is defined as a spiral:

$x_d = 5\sin(0.25t)$ (m);

$y_d = 5\cos(0.25t)$ (m);

$z_d = 0.25t + 0.5$ (m).

The psi angle is set as $\psi_d = 0$ (rad), and the initial position of the quadrotor is (0.5; 0.5).

System parameters of the quadrotor:

1. Mass: m =1.776 (kg).
2. Gravitational acceleration: $g = 9.81$(m/s^2).
3. Thrust coefficient: k_T= 0.0087 (N·s^2).
4. Drag torque coefficient: $k_d = 55{\cdot}10^{-6}$ (N·m·s^2).
5. Arm length: $L = 0.225$ (m).
6. Moment of inertia about x-axis: $I_{xx} = 0.0035$ (kg·m^2).
7. Moment of inertia about y-axis: $I_{yy} = 0.0035$ (kg·m^2).
8. Moment of inertia about z-axis: $I_{zz} = 0.0055$ (kg·m^2).
9. Rotor inertia: $J = 2.8{\cdot}10^{-6}$ (kg·m^2).
10. Drag coefficients: $k_{cx} = k_{cy} = k_{cz} = 5.567{\cdot}10^{-4}$ (N·s/m); $k_{d\Phi} = k_{d\theta} = k_{d\psi} = 5.567{\cdot}10^{-4}$ (N·m·s^2).
11. The parameters of the controller: $c_x = c_y = c_z = 1.55$; $c_\Phi = c_\theta = c_\psi = 10$; $k_x = k_y = k_z = 0.75$; $k_\Phi = k_\theta = k_\psi = 100$; $n_x = n_y = n_z = 1$; $n_\Phi = n_\theta = n_\psi = 1$.

5. 3. Simulation results with a spiral-shaped reference trajectory

The simulation results of trajectory tracking along the coordinate axes are presented in Fig. 2, *a*–*c*.

The simulation results of payload swing angles are shown in Fig. 3, *a*, *b*.

When following the spiral reference trajectory, due to differences in initial states, it takes a short time for the quadrotor to converge to the desired trajectory. Specifically, the x-axis converges in about 2.6 seconds, the y-axis in about 1.5 seconds, and the z-axis in about 2.5 seconds. During this initial period, the payload exhibits larger oscillations, as illustrated in Fig. 3, *a*, *b*. Afterward, the system becomes more stable. However, due to the nature of the spiral trajectory, the suspended payload continues to oscillate in accordance with the quadrotor's motion.

The simulation results of the quadrotor trajectory with a suspended load using a cable are presented in Fig. 4.

In Fig. 4, the quadrotor trajectory and suspended payload motion are depicted more clearly. At the beginning, the payload oscillates significantly, but these oscillations gradually decrease as the quadrotor reaches steady-state flight.

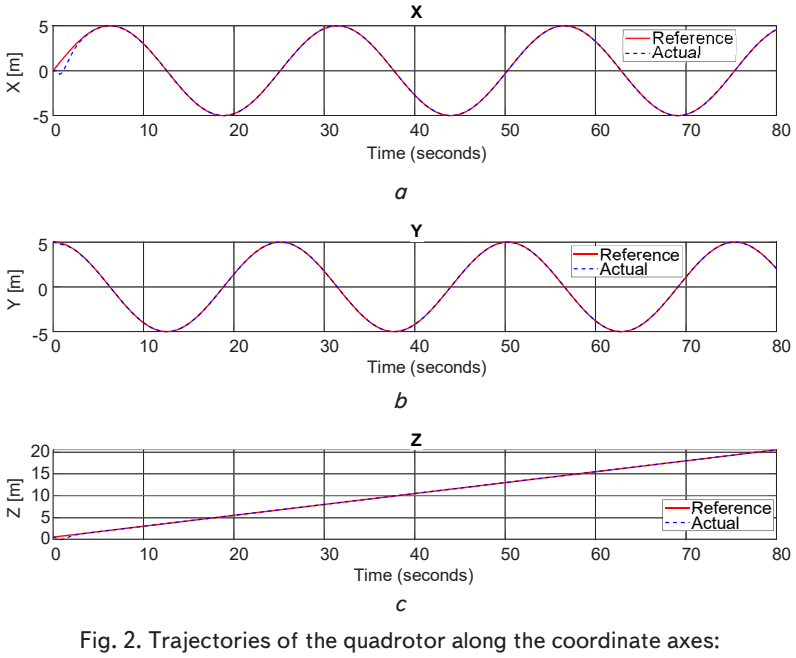

Fig. 2. Trajectories of the quadrotor along the coordinate axes: *a* – quadrotor trajectory along the x-axis; *b* – quadrotor trajectory along the y-axis; *c* – quadrotor trajectory along the z-axis

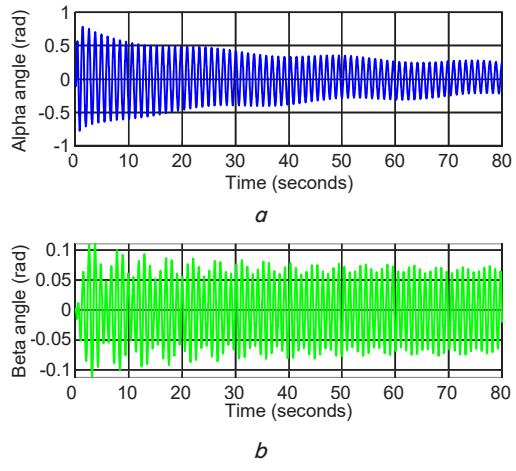

Fig. 3. Oscillation angles of the payload: *a* — swing angle Alpha; *b* — swing angle Beta

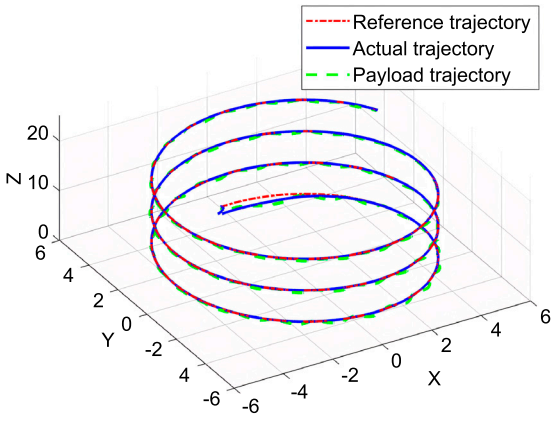

Fig. 4. Trajectories of the quadrotor and the payload

6. Discussion of study results of quadrotor with fixed-length cable suspension

The proposed algorithm, which integrates a SMC with an ESO. In contrast to [5, 6], where often struggle with controlling quadrotors under continuous load oscillations, this result synergistic approach effectively overcomes these limitations and accurately guides the quadrotor along its desired trajectory.

A key advantage of our algorithm is its ability to almost entirely suppress load oscillations (Fig. 3), while the load oscillation error in [15, 16] remains relatively large. The quadrotor accurately tracks its path with near-zero error, converging in approximately 2.6 seconds (Fig. 2), whereas the stabilization time reported in [16] is 3.0 seconds, in [18] is 3.5 seconds, and in [19] is 3.9 seconds. This indicates that the quadrotor employing the proposed algorithm achieves stabilization 13.33% faster compared to [16]. This is made possible by the SMC, which maintains system stability against disturbances, and the ESO, which estimates unknown states. In contrast to a standalone SMC (Fig. 2, 4), which often fails to ensure the Euler angles converge to zero during motion (as in documents [15–17]), our combined solution effectively mitigates this common issue.

The accuracy of our algorithm is further highlighted by the negligible trajectory deviations shown in Fig. 4, all converging to near zero in just 2.6 seconds. While prior studies have often failed to achieve this level of precision. In contrast, previous studies did not achieve this level of precision. The convergence times to zero reported in [18–21] are 3.2 seconds, 3.4 seconds, 3.6 seconds, and 3.5 seconds, respectively. Our algorithm provides a robust solution for quadrotors carrying suspended loads, enabling effective operation under varying conditions.

Despite these strengths, studying has certain limitations. The suspended load is modeled as a pendulum, and a complete elimination of load oscillations has not been achieved. While the algorithm ensures stable operation by keeping oscillation angles within acceptable limits, this research has only been validated through simulations. A crucial next step is to conduct experimental testing, a process that requires significant resources and presents substantial engineering challenges.

Future research will focus on developing a controller for a quadrotor with a suspended load of variable cable length, an endeavor that will require specialized hardware and is expected to have high implementation costs.

7. Conclusions

1. This study successfully developed a novel control algorithm by combining a sliding mode controller with an extended state observer. The algorithm directly addresses a significant gap in existing research by enabling accurate control of a quadrotor with a cable-suspended load to follow a predefined flight trajectory.

2. The proposed model allows the implementation of the algorithm to control a quadrotor with a cable-suspended load flying along a spiral trajectory while operating under varying environmental conditions.

3. A key achievement is the algorithm's capability to accurately control a quadrotor with a fixed cable-suspended load, achieving near-zero error. Quantitative results show that the error becomes negligible within only 2,6 seconds of control, representing a considerable improvement over previous methods, which failed to suppress load oscillations during quadrotor operation. The superior performance of the algorithm is attributed to its simple structure, high convergence rate, and exceptional stability. These features not only ensure its practicality for real-world implementation but also enable it to meet the stringent requirements of unmanned aerial vehicles operating in diverse and complex environments.

Conflict of interest

The authors declare that they have no conflict of interest in relation to this study, whether financial, personal, authorship or otherwise, that could affect the study and its results presented in this paper.

Financing

The study was performed without financial support.

Data availability

The manuscript has no associated data.

Use of artificial intelligence

The authors confirm that they did not use artificial intelligence technologies when creating the current work.

References

1. Lin, S., Liu, A., Wang, J., Kong, X. (2022). A Review of Path-Planning Approaches for Multiple Mobile Robots. Machines, 10 (9), 773. https://doi.org/10.3390/machines10090773
2. Loganathan, A., Ahmad, N. S. (2023). A systematic review on recent advances in autonomous mobile robot navigation. Engineering Science and Technology, an International Journal, 40, 101343. https://doi.org/10.1016/j.jestch.2023.101343
3. Liu, Y., Wang, S., Xie, Y., Xiong, T., Wu, M. (2024). A Review of Sensing Technologies for Indoor Autonomous Mobile Robots. Sensors, 24 (4), 1222. https://doi.org/10.3390/s24041222
4. Niloy, Md. A. K., Shama, A., Chakrabortty, R. K., Ryan, M. J., Badal, F. R., Tasneem, Z. et al. (2021). Critical Design and Control Issues of Indoor Autonomous Mobile Robots: A Review. IEEE Access, 9, 35338–35370. https://doi.org/10.1109/access.2021.3062557
5. Sousa, R. B., Sobreira, H. M., Moreira, A. P. (2023). A systematic literature review on long-term localization and mapping for mobile robots. Journal of Field Robotics, 40 (5), 1245–1322. https://doi.org/10.1002/rob.22170
6. Kabir, H., Tham, M.-L., Chang, Y. C. (2023). Internet of robotic things for mobile robots: Concepts, technologies, challenges, applications, and future directions. Digital Communications and Networks, 9 (6), 1265–1290. https://doi.org/10.1016/j.dcan.2023.05.006
7. Gielis, J., Shankar, A., Prorok, A. (2022). A Critical Review of Communications in Multi-robot Systems. Current Robotics Reports, 3 (4), 213–225. https://doi.org/10.1007/s43154-022-00090-9
8. Garaffa, L. C., Basso, M., Konzen, A. A., de Freitas, E. P. (2023). Reinforcement Learning for Mobile Robotics Exploration: A Survey. IEEE Transactions on Neural Networks and Learning Systems, 34 (8), 3796–3810. https://doi.org/10.1109/tnnls.2021.3124466
9. Orr, J., Dutta, A. (2023). Multi-Agent Deep Reinforcement Learning for Multi-Robot Applications: A Survey. Sensors, 23 (7), 3625. https://doi.org/10.3390/s23073625
10. Sun, H., Zhang, W., Yu, R., Zhang, Y. (2021). Motion Planning for Mobile Robots – Focusing on Deep Reinforcement Learning: A Systematic Review. IEEE Access, 9, 69061–69081. https://doi.org/10.1109/access.2021.3076530
11. Zhu, K., Zhang, T. (2021). Deep reinforcement learning based mobile robot navigation: A review. Tsinghua Science and Technology, 26 (5), 674–691. https://doi.org/10.26599/tst.2021.9010012
12. Cohen, S., Agmon, N. (2021). Recent Advances in Formations of Multiple Robots. Current Robotics Reports, 2 (2), 159–175. https://doi.org/10.1007/s43154-021-00049-2
13. Rafai, A. N. A., Adzhar, N., Jaini, N. I. (2022). A Review on Path Planning and Obstacle Avoidance Algorithms for Autonomous Mobile Robots. Journal of Robotics, 2022, 1–14. https://doi.org/10.1155/2022/2538220
14. Cho, S. W., Park, H. J., Lee, H., Shim, D. H., Kim, S.-Y. (2021). Coverage path planning for multiple unmanned aerial vehicles in maritime search and rescue operations. Computers & Industrial Engineering, 161, 107612. https://doi.org/10.1016/j.cie.2021.107612
15. Omar, H. M., Akram, R., Mukras, S. M. S., Mahvouz, A. A. (2023). Recent advances and challenges in controlling quadrotors with suspended loads. Alexandria Engineering Journal, 63, 253–270. https://doi.org/10.1016/j.aej.2022.08.001
16. Liang, X., Yu, H., Zhang, Z., Liu, H., Fang, Y., Han, J. (2023). Unmanned Aerial Transportation System With Flexible Connection Between the Quadrotor and the Payload: Modeling, Controller Design, and Experimental Validation. IEEE Transactions on Industrial Electronics, 70 (2), 1870–1882. https://doi.org/10.1109/tie.2022.3163526
17. Huang, J., Tao, H., Wang, Y., Sun, J.-Q. (2023). Suppressing UAV payload swing with time-varying cable length through nonlinear coupling. Mechanical Systems and Signal Processing, 185, 109790. https://doi.org/10.1016/j.ymssp.2022.109790
18. Xinyu, C., Yongsheng, Z., Yunsheng, F. (2020). Adaptive Integral Backstepping Control for a Quadrotor with Suspended Flight. 2020 5th International Conference on Automation, Control and Robotics Engineering (CACRE), 226–234. https://doi.org/10.1109/cacre50138.2020.9229913
19. Van Trieu, P., Cuong, H. M., Dong, H. Q., Tuan, N. H., Tuan, L. A. (2021). Adaptive fractional-order fast terminal sliding mode with fault-tolerant control for underactuated mechanical systems: Application to tower cranes. Automation in Construction, 123, 103533. https://doi.org/10.1016/j.autcon.2020.103533
20. Basal, M. A. (2025). Advanced Sliding Mode Control with Disturbance Rejection Techniques for Multi-DOF Robotic Systems. Journal of Robotics and Control, 6 (4), 1612–1623. https://doi.org/10.18196/jrc.v6i4.25779
21. Labbadi, M., Boukal, Y., Cherkaoui, M. (2022). Advanced Robust Nonlinear Control Approaches for Quadrotor Unmanned Aerial Vehicle. In Studies in Systems, Decision and Control. Springer International Publishing. https://doi.org/10.1007/978-3-030-81014-6
22. Tokat, S., Fadali, M. S., Eray, O. (2015). A Classification and Overview of Sliding Mode Controller Sliding Surface Design Methods. Recent Advances in Sliding Modes: From Control to Intelligent Mechatronics, 417–439. https://doi.org/10.1007/978-3-319-18290-2_20
23. Liu, J., Wang, X. (2011). Advanced Sliding Mode Control for Mechanical Systems. Springer Berlin Heidelberg. https://doi.org/10.1007/978-3-642-20907-9